

# Compact multi-band (VIS/IR) zoom imager for high resolution long range surveillance

Andrew Bodkin<sup>a</sup>, Andrew Sheinis<sup>a,b</sup>, Jim McCann<sup>c</sup>

<sup>a</sup>Bodkin Design & Engineering, LLC, P.O. Box 81368, Wellesley, MA 02481;

<sup>b</sup>Center for Adaptive Optics, Univ. of Cal. at Santa Cruz, 1156 High St., Santa Cruz CA 95064;

<sup>c</sup>Andorra Optics, 25 Church St., Marlow NH, 03456

## ABSTRACT

The objective of this project is to seamlessly integrate multiple spectral-band focal plane detector arrays into a single multi-band imaging sensor. The resulting product can be applied to a telescope or a microscope, as simply as changing a lens on a camera. The video stream output provides a set of co-registered digital images from a multiple of spectral bands spanning the Visible, NIR, MWIR and LWIR radiation regions (.4um to 14um). These images have a format that is suitable both for direct observation by a human operator and as a data feed for Automated Target Recognition (ATR) algorithms.

**Keywords:** Surveillance, infrared, multi-band, MWIR, LWIR, NIR, camera, seeker, sensor fusion

## 1. INTRODUCTION

There are numerous electro-optic imaging techniques in use today to accurately locate, identify and characterize objects in the natural environment. For military systems this is important to automatically identify targets, conduct search and rescue, and penetrate darkness for night operations.

Sophisticated sensor systems often consist of a suite of sensors collecting data in a variety of wave bands, and with a variety of techniques. They can include Visible, Infrared, Ladar, Hyperspectral, Polarimetry, MMW, etc. These systems are often co-registered and mounted on a single gimbal in order to give in-depth signature of possible targets and to aid in their identification and discrimination from background and clutter. The compact multipurpose sensor module that is demonstrated here will permit the rapid construction of these types of sensor suites at a fraction of the cost. The mix and match modules will allow various band imagers and active systems to be assembled in a rapid, bolt-together, configuration. In this program we have demonstrated this concept with a dual-band LWIR and visible zoom imager. Future work will demonstrate an additional MWIR channel, a hyperspectral channel, reduce the overall size and weight, and develop a group of compact interchangeable fore-optics

The objective of this program is to assemble the best possible properties from the currently available imaging technologies into a single imaging module. The sensor module will mate the selected sensor arrays together to provide a detection subsystem with a single entrance aperture. Broadband fore-optics are developed to couple the sensor module to the environment with the required resolution and field of view.

The interchangeable design will allow the exchange of detectors arrays and fore-optics. This will permit the upgrade of the system with new technologies as they become available, and the application of the system to various reconnaissance requirements. Future array technologies include hyperspectral imaging, polarization sensitive pixels, two-color pixel arrays, and high density arrays.

The developed product will become a building block for numerous multi-band applications including missile seekers, vehicle mounted imagers, stationary imagers, and airborne reconnaissance systems.

## 2. DESIGN

The system has a common optical input that accepts a wide-band image from a conventional (moderate F-number) reflective fore-optic. The ability of this subsystem to accept input from any reflective (broadband) telescope is a unique and patent pending feature. It permits the interchange of simple, low cost, fore-optics to vary the field of view in order to match the application.

The input from the common optic creates a real image that is split by a dichroic filter and relayed to multiple focal planes. The relay optics are needed to condition the light cone to match the detector requirements. In the LWIR the detector requires an F/1 image cone, in the MWIR the detector needs F/2.3 and in the visible the f-cone is not critical.

The f-cone is conditioned by changing the relay magnification. In the prototype design an all reflective Cassegrain telescope fore-optic is used to create an f/3 intermediate image. The F/3 design is about the limit that can be easily manufactured in a Cassegrain design. The intermediate image created by the fore-optic is split and relayed to the FPAs. In the LWIR channel the relay optics reduce the image size, thus decreasing the f-number, and providing the F/1-cone required by the LWIR detector.

The system has an interface where the detector module mates with the fore-optic. The detector module input consists of an image plane and an acceptance angle (input f-number). At that image plane resides the overlapped real images of the various detector arrays in the system. Thus the relay system creates a virtual focal plane at the fore-optic interface. Changing the focal length of the fore-optic will change the magnification of the image projected on to this virtual focal plane. Likewise changing the magnification of the relays will also change the magnification of the virtual focal plane. In the demonstration system a zoom relay was used to effect a continuous magnification change.

### 2.1 Wave bands

The effective wavelength coverage for optical imaging devices in the field is limited by several factors. The two most important factors are atmospheric absorption (primarily OH absorption by water) and the inherent efficiency of the detector materials. The atmosphere provides good transmission in the following windows: 0.3-1.38, 1.5-1.8, 2.0-2.5, 3.0-4.2, 4.0-4.5, and 7.5-14 microns. Typical detector materials are sensitive in the following bands: Visible (0.3 to 0.7 um Silicon), Near IR (0.7-1.1 um InGas), MWIR (2.0-5.0 um InSb) and LWIR (7.0-14.0 um Microbolometer).

The visible and near IR band provides readily understandable images similar to human vision. These images rely on reflected light for illumination. Therefore they cannot operate at night and are easily deterred by smoke, camouflage and clutter. The infrared bands, on the other hand, can cut through these obscurants. There are two common IR bands available, the Mid-Wave Infrared (MWIR) and the Long Wave Infrared Band (LWIR).

The LWIR extending from 7 – 14 um, also known as the thermal band, is predominantly used to detect room temperature objects by their infrared self-emission. As is shown in figure 1, room temperature objects (from -40° to 80° F) have a predominant blackbody self-emission around 10 um wavelength. This is exceptionally useful for seeing targets in complete darkness, and for seeing through smoke and camouflage such as netting and paints.

MWIR is superior in some ways to LWIR in the fact that the diffraction limited resolution is much greater, by as much as 2.5 times. The detector technology is less noisy providing higher sensitivity, and easing the f/number requirement. Also, there is considerable solar radiation available in the MWIR adding reflected light to the self emitted radiation. On the other hand the detectors are cryo-cooled, requiring a cooling compressor, and the arrays are at least 3 times the cost of LWIR microbolometers.

The effective image resolution for these systems will be limited by one of several factors, depending on the wavelength band. These factors include: aberrations in the optical system, detector pixel resolution, optical diffraction, and aberrations induced by atmospheric turbulence. In a multi-band system, the importance of these factors in limiting the resolution will vary depending on the waveband.

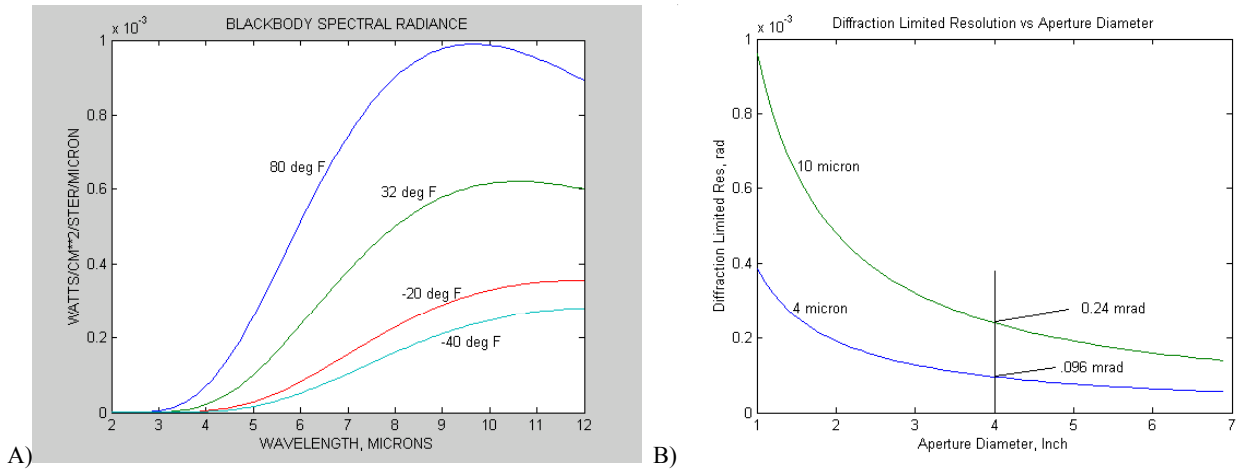


Figure 1: A) Shows the black body curve of a near room temperature object, the peak of the self-emission is in the LWIR band (7-14 um). B) Although there is less self-emission in the MWIR (3-4 um) the spatial resolution, as determined by the diffraction limit, is 2.5 times better than in the LWIR (graphs courtesy of L. Wilkins, NAVAIR).

The resolution of the system is limited by atmospheric turbulence in the visible band, and diffraction limited in the LWIR band. This is because the diffraction limited spot size increases linearly with wavelength ( $\sim\lambda/d$ ) while the turbulence induced blur-spot size decreases as wavelength to the 1/5<sup>th</sup> power. For a 12 inch aperture, the visible turbulence blur spot is  $\sim 5$  to 20 urad, and in the LWIR it is  $\sim .4$  to .1 urad. Whereas the diffraction limited spot is 1.6 urad in the Visible, and 28 urad in the LWIR. Active and adaptive optical systems are sometimes employed to extend the practical resolution limit beyond that imposed by the atmosphere.

## 2.2 Target Detection

Target detection is determined by how big the target is in the image and how many pixels it covers in the array. If it covers lots of pixels the target can be easily identified, if only a few, the target might be overlooked.

In order to determine the detection limit for the LWIR channel we have adopted a modified Johnson criteria. A target such as a SCUD missile is estimated to be 40 ft by 10 ft in length. This results in a characteristic length of  $(40 \times 10)^{.5} = 20$  ft. This characteristic length is mapped onto pixels with the lens system. To “ID” the target the characteristic length must equal 16 pixels; to “recognize” the target, 8 pixels; to “detect” the target, 4 pixels. This criteria only applies when the system resolution is pixel limited, if it is optics limited then the pixel should be replaced with the length of the resolution element.

Table 2: The characteristic length is calculated for a SCUD from above and a “man” from the side. The characteristic length is used to determine the required pixel footprint.

	Length	Width	Characteristic length	Pixel footprint		
				ID	Recognize	Detect
				16	8	4
	ft	ft	ft	ft	ft	ft
Scud	40	10	20	1.25	2.5	5
Man	6	2	3.5	0.22	0.43	0.87

The data from Table 2 is converted to pixel field of view (PFOV), as dependent on range to target in Table 3. Global Hawk, Predator and Tower are typical applications; their associated ranges are listed.

Table 3: Detection criteria at various ranges.

		range (ft)	PFOV		
			ID	recog	detect
			urad/pix	urad/pix	urad/pix
Scud	Global hawk	65000	19	38	77
	Predator	25000	50	100	200
Man	Global hawk	65000	3.3	6.7	13
	Predator	25000	8.7	17	35
	Tower	5000	43	87	173

This data is used in the model shown in Table 4, which lists the detection of a “man” and a SCUD at the ranges of 65,000 ft, 25,000 ft and 5,000 ft. The model assumes the use of the LWIR array with 320 x 240 pixels on a 25 um pitch. It examines four aperture sizes and three f-numbers.

The ratios expressed under the “SCUD” and “Man” headings are the characteristic PFOV from Table 3, divided by the PFOV as determined by the aperture size and f-number listed in the table. As an example, the third line shows a 12 inch aperture, operating at f/2. This will just about “recognize” a SCUD from 65,000 ft. (.9), easily “detect “ a SCUD at 25000 ft (1.2) and at 5000 ft, “ID” a man (1.1). The quantities in shaded boxes are the values we consider to be qualifying, which we chose as a ratio of (.9) or greater.

Table 4: Detection threshold for various magnification systems. Detection ratio >.9 is qualifying.

		Detection Ratio										FOV	
Aperture	F#	PFOV	SCUD						Man			Horiz. deg	Vert. deg
			65000			25000			5000				
in		urad	ID	recog	detect	ID	recog	detect	ID	recog	detect		
12	1.0	82.0	0.2	0.5	0.9	0.6	1.2	2.4	0.5	1.1	2.1	1.50	1.13
12	1.5	54.7	0.4	0.7	1.4	0.9	1.8	3.7	0.8	1.6	3.2	1.00	0.75
12	2.0	41.0	0.5	0.9	1.9	1.2	2.4	4.9	1.1	2.1	4.2	0.75	0.56
8	1.0	123.0	0.2	0.3	0.6	0.4	0.8	1.6	0.4	0.7	1.4	2.26	1.69
8	1.5	82.0	0.2	0.5	0.9	0.6	1.2	2.4	0.5	1.1	2.1	1.50	1.13
8	2.0	61.5	0.3	0.6	1.3	0.8	1.6	3.3	0.7	1.4	2.8	1.13	0.85
6	1.0	164.0	0.1	0.2	0.5	0.3	0.6	1.2	0.3	0.5	1.1	3.01	2.26
6	1.5	109.4	0.2	0.4	0.7	0.5	0.9	1.8	0.4	0.8	1.6	2.01	1.50
6	2.0	82.0	0.2	0.5	0.9	0.6	1.2	2.4	0.5	1.1	2.1	1.50	1.13
4	1.0	246.1	0.1	0.2	0.3	0.2	0.4	0.8	0.2	0.4	0.7	4.51	3.38
4	1.5	164.0	0.1	0.2	0.5	0.3	0.6	1.2	0.3	0.5	1.1	3.01	2.26
4	2.0	123.0	0.2	0.3	0.6	0.4	0.8	1.6	0.4	0.7	1.4	2.26	1.69

Two significant conclusions can be drawn from this table. The first is that the ability to recognize a target is primarily dependent on the aperture of the telescope. Second is that as the f-number increases, the ability to recognize targets also increases. Unfortunately, the larger the f-number the less signal arrives at the detector, and in this case of the microbolometer the amount of noise in the image greatly reduces the ability to identify targets.

### 2.3 System Design

The prototype system consists of two detector focal planes mated through a dichroic beam splitter, sharing input from a common Cassegrain fore-optic (figure 2). The beam splitter is in the converging beam of the fore-optic and divides the primary input into two intermediate images. Each image has corrector optics that increase the usable FOV. Each channel has its independent zoom assembly that is controlled by a central processor. The visible leg uses a commercial zoom assembly and a servo control board. The custom LWIR channel has two moving elements and uses stepper motor drives.

The optical design criterion for this system was to expand the corrected field of view (FOV) of the Cassegrain telescope, which is typically 0.5 degrees. Requirements for the imaging system were up to 4 degrees full FOV. To further challenge the designer, the bandpass requirement was to simultaneously image the VIS/NIR (0.4 to 1.0  $\mu\text{m}$ ) and LWIR (8 to 12  $\mu\text{m}$ ).

The design problem was originally conceived as a single problem for both bandpass windows. An excellent design was achieved using a three-element corrector at the field plane of the telescope to correct both the field aberrations (primarily coma) and to control the color induced by the corrector over a wide field of view (4 degrees) and wide free spectral range (0.4 to 12  $\mu\text{m}$ ). However the task of producing an anti-reflective coating that covered this band turned out to be insurmountable. As an alternative it was decided to correct the visible and IR beams separately post beam-splitter. The task then became separable at the image plane relay, i.e. the visible and LWIR images were separated by a beamsplitter to individual optical channels for each bandpass. Each channel then contained its own corrector and variable magnification relay.

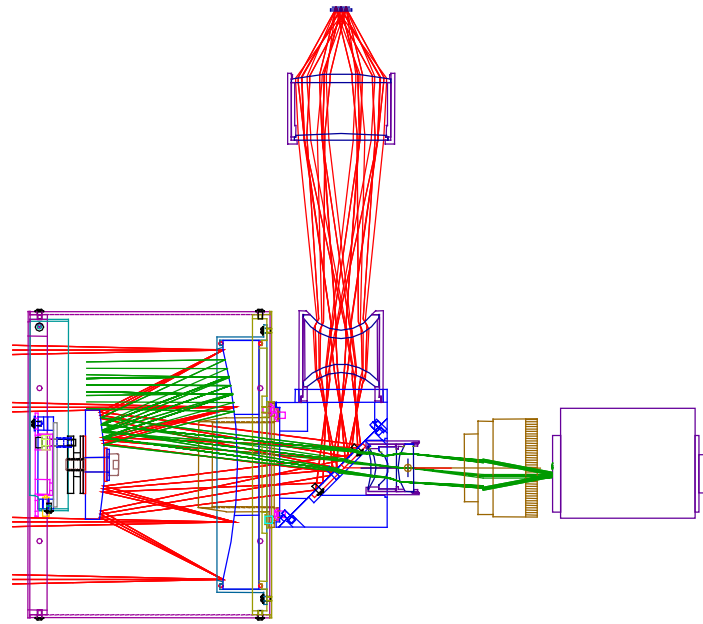


Figure 2: The system assembly showing Cassegrain fore-optics, dichroic beam splitter, and correctors for both channels. The IR channel uses a custom zoom and the visible channel uses off-the-shelf commercial zoom.

## 2.4 Infrared Optics

The infrared portion of the system passes through a 4 element zoom as shown in Figure 2. This subsystem consists of all germanium elements with one hybrid diffractive/asphere surface. The basic layout consists of a fixed two element corrector shown just past the fore-optic's intermediate image and a movable two-element variator group to provide the re-imaging<sup>3</sup>. The zoom range is continuous from F/1 to F/3 and is accomplished with 2 motorized motions. The variator group is moved over a 100 mm range to accomplish the magnification and the detector is moved over a 28 mm range to follow the image. Since the fore-optics are F/3 the zoom ratio is three to one.

The fixed group's primary function is to redirect the chief rays from the fore-optic into the variator elements and provide some aberration correction to the wavefront. The redirection essentially reimages the exit pupil of the fore-optic to a position just beyond the 2<sup>nd</sup> variator element (figure 3). At F/1 the curvature of the 2<sup>nd</sup> element becomes fairly steep to compensate the fore-optics large field curvature and astigmatism at the edge of the field. The intermediate image ranges from a diagonal dimension of 11.2 mm at F/3 to 33.6 mm at F/1.

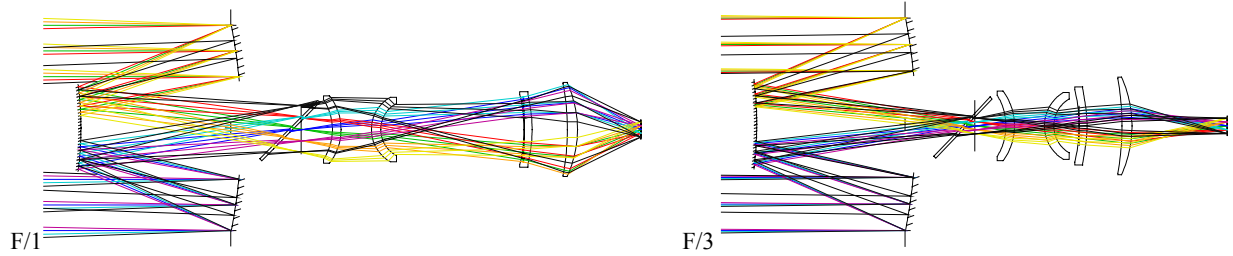


Figure 3: Preliminary zoom assembly design for the prototype. The zoom range is shown with F/1 on the left, and F/3 on the right. This design has a straight through IR path, in the as-built system the IR zoom path reflects off a 45 degree beamsplitter placed after the fore-optic

The hybrid diffractive/aspheric is on the concave surface of the 1<sup>st</sup> variator element. This arrangement of combining the diffractive correction with the asphere is possible by the use of diamond turning. This allows the design to minimize the number of special surfaces and keeps the system cost-effective. Alignment sensitivity is reduced as all the precision is placed into the one diamond turned surface eliminating the need to align multiple aspheres.

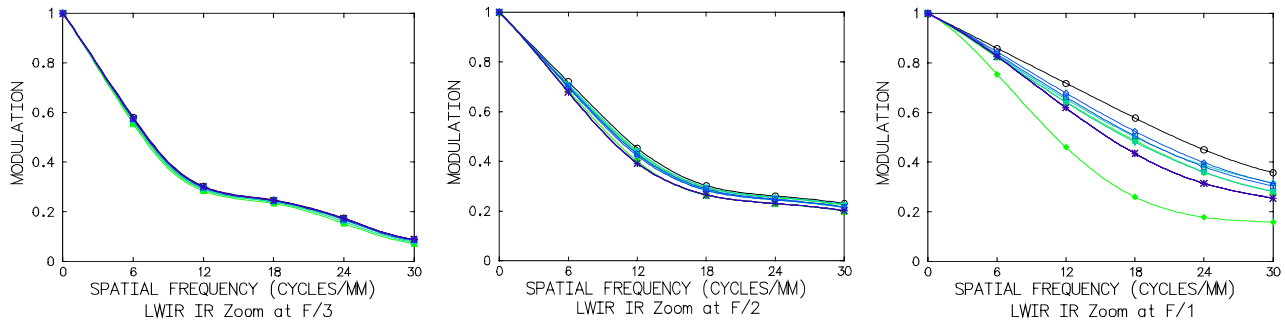


Figure 4: MTF curves for the IR zoom relay for F/1, F/2 and F/3 respectively from left to right. The cutoff frequencies are 100 LP/mm at F/1, 50 LP/mm at F2 and 33 LP/mm at F/3. The pixel limited cut-off for the array is at 18 lp/mm

Figure 4 shows the MTF performance curves over the FOV, wavelength and zoom range. The final design performance is essentially diffraction limited over this entire range. The cutoff frequencies are given by the expression  $f_c = 1/(\lambda F/\#)$  in line pairs per mm. Thus at a center wavelength of 10 microns they are 100 LP/mm for F/1, 50 LP/mm at F/2 and 33 LP/mm at F/3. The dip in the MTF curve at the middle frequencies is caused by the fore-optics obscuration.

Although germanium has low dispersion in the LWIR band of 7-14 microns, at F/1 the longitudinal color begins to dominate the aberration contribution. This necessitates either another type of material in a negative power element or a diffractive surface which can provide the required negative dispersion. As the desire is to keep the number of elements to a minimum and the variator elements positive, the diffractive surface gives a good solution.

Figure 5 is the distortion over the FOV for the extreme zoom positions. This type of distortion is pincushion with a maximum of 2.5% in the corner at F/1. Other than the fore-optic obscuration, there is essentially no vignetting in this design.

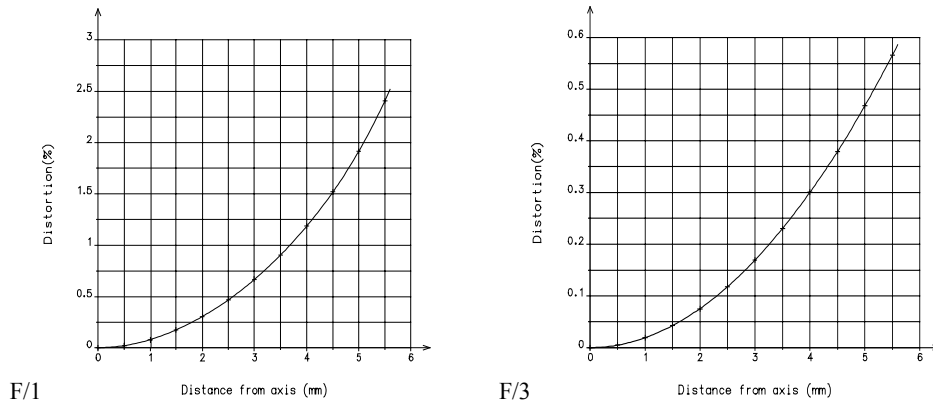


Figure 5: Distortion plots for the zoom lens at F/1 and F/3

To correct the color at F/1 and to control higher order aberration, one surface is made into a diffractive asphere. This occurs on the convex surface of the 1<sup>st</sup> variator element. Since the surface can be diamond turned, it is possible to combine the diffractive profile with the aspheric “cap” and have them machined accurately in one setup.

The diffractive surface works by having an intrinsic dispersion that is linear with wavelength and in the opposite sense, i.e., negative, with respect to refractive materials. Therefore we can combine this negative dispersion from the surface with the positive dispersion of the germanium elements to create a color compensating system over the wavelength range<sup>3</sup>.

Figure 6 shows the radial cross section of the hybrid surface sag. This particular surface has a base radius of curvature, a conic constant, higher order aspheric terms to 10<sup>th</sup> order and the diffractive phase profile all in one definition. The overall shape of the lens is measured in millimeters. The aspheric bell shape of the lens drops almost a full millimeter in height along its 30mm radius. Into this surface is cut a diffractive curve, consisting of three ridges. Too fine to see on the same scale, the diffractive sag is measured in microns.

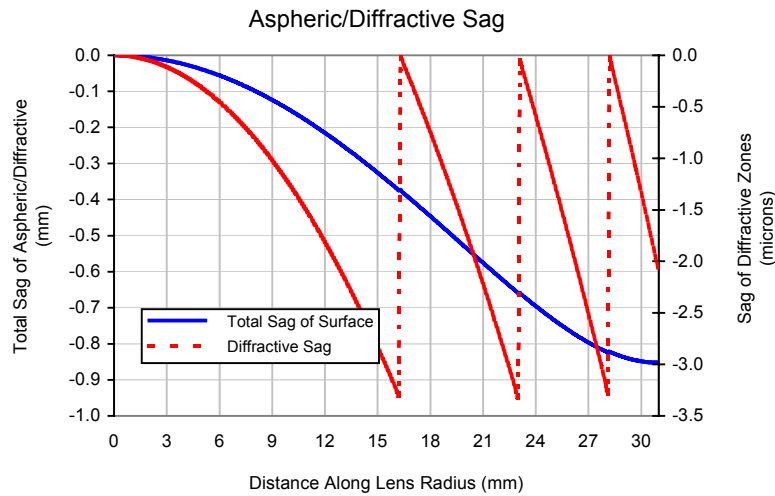


Figure 6: Aspheric and diffractive sag. The overall shape of the lens is measured in millimeters (solid line, left scale). The aspheric bell shape of the lens drops almost a full millimeter in height along its 30mm radius. Into this surface is cut a diffractive curve, consisting of 3 minute ridges, (dotted line, right scale). Too fine to see on the same scale, the diffractive sag is measured in microns

Since the dispersion of germanium is small, the “power” of the diffractive surface is small and consists of only 4 distinct zones. This is in contrast to some diffractives for the visible wavelength region that can have thousands of zones over the same radial dimension. In this design there is only the 2<sup>nd</sup> order phase term from the diffractive profile since we only need to correct primary color with it. The aspheric portion of the surface is used to correct the 3<sup>rd</sup> and higher order aberrations.

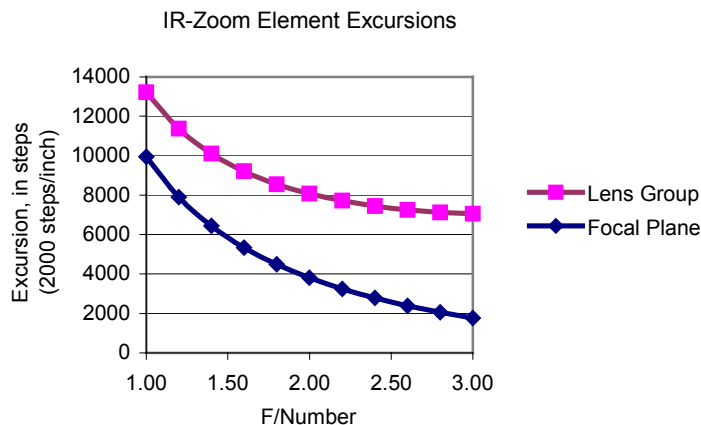


Figure 7: The displacement of the focal plane and the zoom group. The relative difference in their position increases linearly with f-number (zoom magnification). A control algorithm is used to move both elements via independent stepper motor drive.

The IR system has two moving elements, the focal plane and the adjacent two element group. These are moved to effect a zoom according to the displacement shown in figure 7. The assemblies are carried on linear bearing with two guide rods. Each assembly has three linear bearings and an adjustable tensioner so the residual play in the bearings can be eliminated. A microcontroller is used to drive the stepper motors and position the elements. The destination position for each of the two traveling components at the end of a “move” command is done with a discrete look-up table and linear interpolation. The look-up tables are designed for infinite focus. For closer targets a variable offset is added. Once focused on the target, the system will maintain focus through a zoom operation.

## 2.5 Visible optics

The primary requirement behind the visible design was to use off-the-shelf optics wherever possible. In order to use an off-the-shelf optic to relay the visible image we had to first correct the fore-optic aberration. A commercial camera lens was used as a collimator and a commercial zoom lens as the final imager. This achieves a variable magnification over a relatively large FOV. In order to avoid vignetting, the fore-optic pupil was imaged onto the zoom lens entrance pupil.

The fore-optic aberrations in the visible path were well corrected over the 4 degree FOV by a 3 element zero-power corrector. A zero-power corrector has the advantage that, it requires the use of identical glass for all corrector elements to produce zero chromatic aberration. This would result in an easily fabricated corrector, but in order to condition the pupil going into the collimator a powered corrector is required. This requirement results in the trade-off of distortion and chromatic aberration induced at the corrector against vignetting in the system.

The results of the final lens design are shown in figure 8. The distortion is low, under 0.5% and the MTF is matched at the array cut-off at 67 lp/mm.

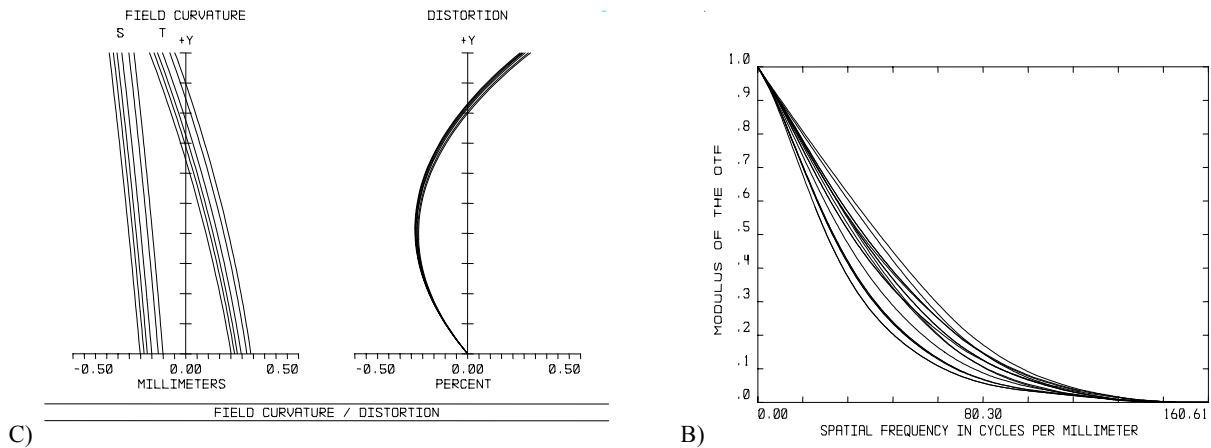


Figure 8: A) Shows the field curvature and distortion plots. Distortion is under 0.5%. B) Shows the MTF for the system over the field-of-view. The array cut-off is at 67 lp/mm which has roughly 20% modulation, a reasonable match for the system.

## 2.6 Demonstration test bed

A demonstration unit has been built and tested, and is shown in figure 9. This system, called the “Omni Spotter” provides LWIR imagery from a microbolometer array and high sensitivity visible imagery from a silicon CCD using Sony HyperHAD technology (figure 10). The IR system has a continuous zoom from 4 degrees to 1.3 degrees (figure 11). The system is designed to operate at long range from 1 to 20 km.

The signals from the two focal plane arrays are available in both analog and digital format. Analog signals are NTSC compliant and are accessed via camera body connector. A built in video server digitizes these video streams and permits viewing of the data through the internet. Control of pan/tilt zoom and focus may also be accessed through the internet portal.

The LWIR zoom module is removable and can be operated as a stand alone channel. A set of fore-optics has been designed to provide a wide range of magnifications for the module, from 36° to 1.3° field-of-view.



Video Out: NTSC Composite, Digital, Internet Protocol
Power In: 1 W, 12 VDC
Spectral Bands:
8-14 um
400-1100 nm
Detection Modules:
IR: 320 X 240 Pixels
Vis: 420 lines, 10-bit digital
Sensitivity: IR: <50 mK MRTD
Vis: 0.0003 Lux
Field of View: Zoom 4°-1.3°
Dimensions: 8.0" W x 18.0" H x 22" L
Weight: <20 lbs.

Figure 9: Omni Spotter test bed. This single aperture camera yields two co-aligned fields-of-view in different spectral bands. The camera provides simultaneous 3x zoom in both bands. It has interchangeable fore-optics to change the field-of-view range.

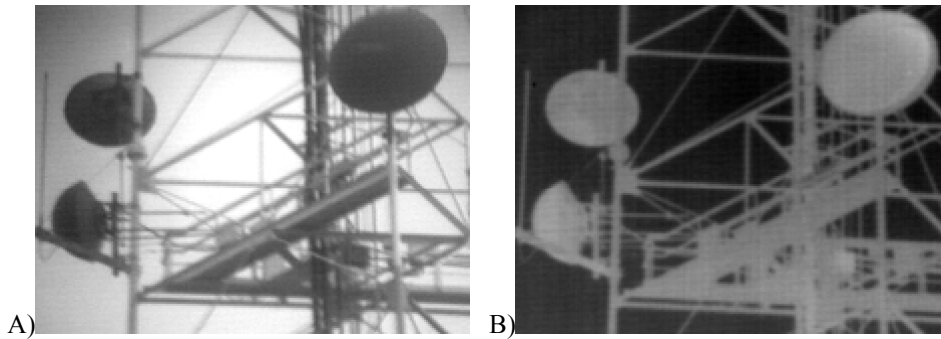


Figure 10: Still video frames taken with the Omni Spotter dual-band camera. A) Visible band. B) LWIR band. The radio tower is at a range of 1000 ft. These images were downloaded from the camera directly through the internet.

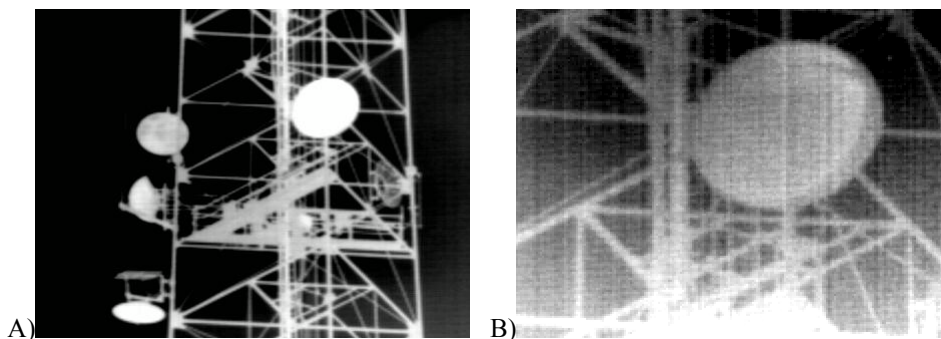


Figure 11: Still video frames showing the 3x infrared zoom. A) Wide field image is 4°. B) Narrow field image is 1.3°. These images were downloaded from the camera directly through the internet.

### 3. CONCLUSIONS

A Dual band sensor suite has been developed and demonstrated. The unique design offers a seamless integration of multiple focal plane technologies. This new approach allows the multi-band system to be treated as a single camera suite, permitting application of various fore-optics, from telescope to microscope.

The interchangeable design permits the exchange of detectors arrays and fore-optics. This simplifies the upgrade of the system with new technologies as they become available, and the adaptation of the system to various reconnaissance requirements

Built and demonstrated was a unique infrared zoom co-aligned with a visible zoom. The system mates the focal planes providing even matching between optics limited and pixel limited resolution. In night time operations the demonstration system, relying on the infrared channel, will be able to recognize a SCUD missile launcher from 25000 ft range, and detect it from 65000 ft. The visible channel provides higher resolution and will improve recognition during daylight operations.

The long wave infrared module provides a unique 3x continuous zoom magnification. The infrared zoom module is designed to stand alone, and has a set of fore-optics with a wide range of magnifications. The module can cover from 36° to 1.3° field-of-view. The output signals are NTSC compliant, and accessed via camera body connector. A built in video server digitizes these video streams and permits viewing of the data through the internet.

The mix and match design will allow various band imagers and active systems to be assembled in a rapid, bolt-together, configuration. In this program we have demonstrated this concept with a dual-band LWIR and Visible zoom imager. Future work will demonstrate adding an additional MWIR channel and a hyperspectral channel, reducing the overall size and weight, and developing a group of compact interchangeable fore-optics

#### 4. ACKNOWLEDGEMENTS

This work was funded by the Naval Air Warfare Center Weapons Division of the U.S. Navy, under contract Number N68936-03-C-0013. The authors wish to thank Dr. Lowell Wilkins for his guidance, encouragement and support.

#### 5. REFERENCES

1. D.L.Fried, Statistics of a Geometric Representation of Wavefront Distortion, *J. Opt. Soc. Am.*, 1965, Volume **55**, p. 1427-1435
2. Sheinis A. I., Cowie L., McKenna D., Micro-Thermal Instrumentation for Haleakala Site Survey, *Adaptive Optics for Large Telescopes: Optical Society of America Topical Meeting*, 1992, Tech digest vol. **19**.
3. M.J. Riedl, J.T. McCann, Analysis and Performance Limits of Diamond Turned Diffractive Lenses for the 3-5 and 8-12 Micrometer Regions., SPIE Critical Reviews Volume 38, 1991.